Excerpt from the Proceedings of the 2011 COMSOL Conference in Boston

Modeling of Galvanic Interactions between AA5083 and Steel Atmospheric Condition

D. Mizuno*[1, 2], Y. Shi[1] and R. G. Kelly[1]
[1]University of Virginia, [2]JFE Steel Corporation
*Corresponding author: Charlottesville, VA 22904, dm3ef@virginia.edu email address

Abstract: Aluminum alloys 5000 series are widely used in naval ships. There is a concern that galvanic interactions will exacerbate corrosion of these aluminum alloys leading to pitting, intergranular corrosion (IGC) and intergranular stress-corrosion cracking (IGSCC), because they are joined via steel fasteners. In this study, a model of the galvanic corrosion between aluminum alloy AA5083 and steel under atmospheric conditions was built. The model geometry was a simple one consisting of the domain of NaCl solution and the boundaries of aluminum and steel surfaces exposed to the solution. The Nernst-Plank equation, with the application of electroneutrality was used to calculate the potential and the current density distributions in a thin electrolyte. The extended Buttler-Volmer equations fitted to the polarization curves were used as the boundary conditions. The potential distribution measured by Scanning Kelvin Probe (SKP) under a thin electrolyte was compared with the model calculation to validate it. The model output had good agreement with the experimental data both in bulk solution and under thin electrolyte conditions.

Keywords.
Nernst-Plank, galvanic corrosion, atmospheric corrosion, Aluminum alloy, AA5083

1. Introduction

AA5XXX alloys are widely used on the cabin of ships and vehicles across the Department of Defense, because they have a good combination of strength, ductility, weldability and corrosion resistance. However, it is well recognized that these materials are susceptible to IGC (Intergranular Corrosion) and IGSCC (Intergranular Stress Corrosion Cracking) due to the sensitization in which β (Al_3Mg_2) phase precipitates along grain boundaries during service. In addition, these aluminum alloys are often joined via steel fasteners. There is thus a concern that galvanic interactions will exacerbate corrosion of the AA5083 leading to pitting, IGC and IGSCC, especially when it is sensitized. Characterization of β phase at grain boundary and computational modeling for predicting IGC damage are being studied in our research group [1].

Galvanic corrosion of aluminum alloys has been widely studied, including with computational modeling. Murer et al. studied micro-galvanic corrosion between aluminum alloy matrix and inter metallic particles [2, 3]. Xiao et al. built a model to predict the pitting on aluminum alloy [4]. However, there are few studies galvanic corrosion of aluminum alloys under atmospheric conditions. It is very hard to experimentally evaluate the galvanic corrosion behavior in atmosphere from experiments in a laboratory due to the existence of numerous important factors including loading density, relative humidity, area ratio of metals and so on. Therefore computational work is believed to be an effective tool to predict atmospheric corrosion.

The main objective of this study is to build the preliminary model to predict the potential and the current density distribution due to the galvanic coupling between AA5083 aluminum alloy and AISI4340 steel under a thin electrolyte to simulate the atmospheric corrosion.

2. Modeling

2.1 Geometry

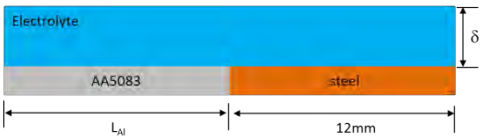

(a) Schematic drawing of model geometry

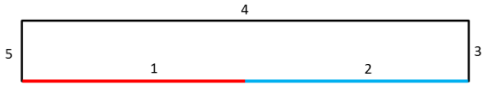

(b) Domain and boundaries in the geometry

Figure 1. Schematic drawing of model geometry.

Fig.1 shows the geometry which was used in this study. It consists of boundaries of two metals and electrolyte. The thickness of electrolyte, δ, should be small to simulate atmospheric conditions. In this study, the minimum value of δ was 0.2mm, because the calculation would not converge when the δ was less than 0.2mm. The length of AA5083 surface, L_{Al} was also changed, keeping the length of steel constant to investigate the influence of the area ratio of two metals. The boundaries 3to 5 were insulators.

2.2 Governing equation

The Nernst-Planck equation with electroneutrality was used for the calculations. The terms for diffusion and migration of species were considered, and convection can be ignored under thin electrolyte. The Nernst-Planck equation for the species *i*, is expressed as follows,

$$\frac{\partial c_i}{\partial t} = \nabla \cdot \left(-D_i \nabla c_i - z_i F \frac{D_i}{RT} \nabla \emptyset\right) = R_i \qquad (1)$$

Where, c_i is the concentration of the species i ($mol \cdot m^{-3}$), D_i is the diffusion coefficient of the species i, z_i is the charge number of the species i, F is the Faraday constant (96500 $C \cdot mol^{-1}$), Φ is the potential in the domain (in the solution) (V vs SCE), R_i is the production term which represents the flux of species due to reactions in the domain ($mol \cdot m^{-2} \cdot s^{-1}$). This equation introduces n+1 variable which are the concentration of each dissolved species and the potential, Φ. The electroneutrality equation was used to eliminate the variable and solve these equations.

$$\sum z_i c_i = 0 \qquad (2)$$

Table 1. Initial concentration and diffusion coefficient for each species in the domain

	Initial Concentration ($mol \cdot m^{-3}$)	Diffusion Coefficient ($m^2 \cdot s^{-1}$)
Na^+	600	1.3×10^{-9}
Cl^-	600	2.0×10^{-9}
H^+	10^{-4}	9.3×10^{-9}
OH^-	10^{-4}	5.3×10^{-9}
Al^{3+}	0	10^{-9}

Table 1 shows the initial concentration and the diffusion coefficient for each species used in this model. The ionic product for water was also considered in the reaction term R_i.

$$R_{H+} = R_{OH-} = k_{wf} - k_{wb} \cdot [H^+] - [OH^-] \qquad (3)$$

k_{wf} and k_{wb} represent the forward and backward rate constants for water respectively. In this study, $k_{wf} = 10^{-4}$ and $k_{wb} = 10^4$ were used. $[H^+]$ and $[OH^-]$ are the concentration of H^+ and OH^- ($mol \cdot m^{-3}$) respectively.

The boundary conditions for the surface of two metals were determined from electrochemical experiments. The current density as the boundary condition is expressed by the equations which consist of the Buttler-Volmer equation and cathodic diffusion plateau.

For the surface of AA5083 (boundary 1):

$$i_{Al0} \cdot \exp((E_{Al0}-(V_m-V))/-\alpha_{Ala}) + i_{AlLim} \cdot i_{Al0} \cdot \exp(\alpha_{Alc} \cdot F \cdot (E_{Al0}-(V_m-V))/R/T)/(i_{AlLim} + i_{Al0} \cdot \exp(\alpha_{Alc} \cdot F \cdot (E_{Al0}-(V_m-V))/R/T)) \qquad (4)$$

i_{Al0} represents the exchange current density for aluminum alloy AA5083. i_{AlLim} is the limiting current density of cathodic reaction on AA5083. E_{Al0} is corrosion potential of AA5083. α_{Ala} and α_{Alc} are charge transfer coefficient of anodic and cathodic reactions. R is gas constant (J/mol/K) and T is temperature (K).

V is the potential of the metal (V) and V_m is the potential in the solution (V). In this study, V_m was set to 0.

For the surface of steel (boundary 2):

$$i_{FeLim} \cdot i_{Fe0} \cdot \exp((\alpha_{Fec} \cdot F \cdot (E_{Fe0}-(V_m-V))/R/T)/(i_{FeLim} + i_{Fe0} \cdot \exp(\alpha_{Fec} \cdot F \cdot (E_{Fe0}-(V_m-V))/R/T)) \qquad (5)$$

i_{FeLim} represents the limiting current density of cathode due to the oxygen diffusion on steel. i_{Fe0} is the exchange current density for steel. E_{Fe0} is the corrosion potential of steel. α_{Fec} is charge transfer coefficient of cathodic reactions on steel. The anodic reaction of steel was not considered in this equation because the influence of it on galvanic corrosion for AA5083 is negligible.

Each parameter in equations (4) and (5) was determined by fitting to experimental polarization curves. **Fig.2** shows the fitting of

these curves. The parameters used equation (4) and (5) as the boundary conditions were shown in **Table 2**.

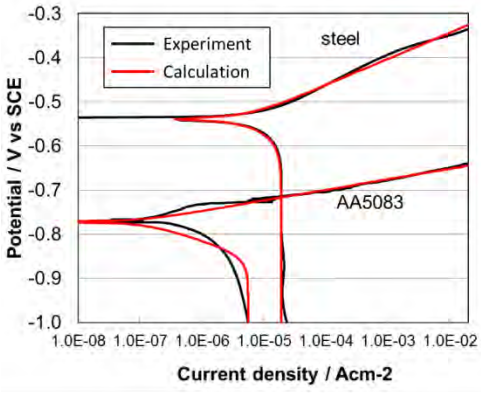

Figure 2 Determination of parameters for boundary conditions from polarization curves.

Table 2 Electrochemical parameters for boundary conditions.

Boundary	type	Parameters				
1	anode	i_{Al0}(A/m^2)	E_{Al0}(V_{SCE})	i_{AlLim}(A/m^2)	α_{Ala}	a_{Alc}
		9.6x10^{-4}	-0.772	-5.6x10^{-2}	2.5	1.5
2	cathode	i_{Fe0} (A/m^2)	E_{Fe0}(V_{SCE})	i_{FeLim} (A/m^2)	α_{Fea}	
		-5.6x10^{-2}	-0.535	-1.9x10^{-1}	1.0	

In bulk electrolyte, the galvanic corrosion was controlled by the reduction reaction of oxygen on the steel surface. The limiting current density, i_{FeLim} was changed as a function of the thickness of electrolyte, increasing when the thickness of electrolyte is thin, because more oxygen dissolved in solution could reach the surface of steel more easily though the thinner diffusion layer. The limiting current density, i_{FeLim} is determined by following equation.

$$i_{FeLim} = zFD_{O2}C_{o2} / \delta \quad (6)$$

Where, D_{O2} is the diffusion coefficient of oxygen, C_{o2} is the concentration of oxygen in solution. In this study, D_{O2}=1.27x10^{-9}(m^2·s^{-1}) and C_{o2}=2.58x10^{-1}(mol·m^{-3}) were used. δ is the thickness of diffusion layer. The value of δ can be deemed to be same as the thickness of the electrolyte when the electrolyte is very thin (0.2 mm or less) like under atmospheric conditions.

Table 3 The flux of chemical species for boundary conditions.

Boundary	Type	Reaction	flux of spieces
1	anodic reaction	$Al \rightarrow Al^{3+} + 3e^-$	$j_{Al3+} = i_a / 3F$
2	cathodic reaction	$O_2 + 2H_2O + 4e^- \rightarrow 4OH^-$	$j_{OH-} = i_c / F$
3-5	electric insulator	—	—

Electrochemical reactions occur on the anode of AA5083 and the cathode of steel during galvanic corrosion. The reactions on anode and cathode are expressed as follows:

$$Al \rightarrow Al^{3+} + 3e^- \quad (7)$$

$$O_2 + 2H_2O + 4e \rightarrow 4OH^- \quad (8)$$

Al^{3+} and OH^- generated by electrochemical reaction in equations (7) and (8) were considered in this model. The flux of these chemical species is determined by the current density flowing on each metal surface. Table 3 shows the flux of chemical species used as the boundary conditions.

3. Experimental

In this study, the potential distribution around the joint between AA5083 and steel under thin electrolyte was measured using the Scanning Kelvin Probe (SKP) to validate our numerical model. SKP is a non-contact technique which can measure the difference of work function between a vibrating reference probe and the specimen. The work function or Volta potential measured by SKP has been found to have a good correlation with the corrosion potential of the surface as measured in bulk solution [5-7]. The specimen consisted of AA5083 aluminum alloy and steel which were connected to each other and embedded in epoxy resin. **Fig.3** shows the appearance of the specimen. In order to define the area ratio, the area except that for measuring surface was covered with insulating lacquer paint. A thin electrolyte layer of 100μm was formed on the surface of the specimen using 0.6M NaCl solution. The specimen was put in a humidity controlled chamber attached to the SKP apparatus, and the relative humidity was kept around 98% during the experiment to maintain the thickness and the concentration of the electrolyte. The potential distribution under 1.0

mm thick electrolyte which can be deemed to almost bulk solution was also measured by SKP.

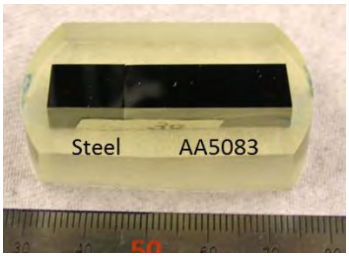

Figure 3 The specimen for SKP measurement.

4. Results

Fig.4 shows the potential distribution under a 1.0 mm thick of 0.6M NaCl solution. The data taken from SKP is also plotted in this Figure. The model calculations show that the potential tends to increase with increasing area ratio of steel. However, the difference of potential between them was slight. In addition, the potential of the entire AA5083 and steel was almost constant regardless of the area ratio. The data for the 1:1 area ratio taken from SKP was also almost constant on the entire surface of specimen and the value of them was very close to the calculation result. **Fig.5** shows the current density distribution under a 1.0mm thick of 0.6M NaCl solution. The anodic current density on AA5083 increased with increasing area of steel. However, for each area ratio, the current density on the entire AA5083 surface was almost constant, although that around the boundary was slightly higher.

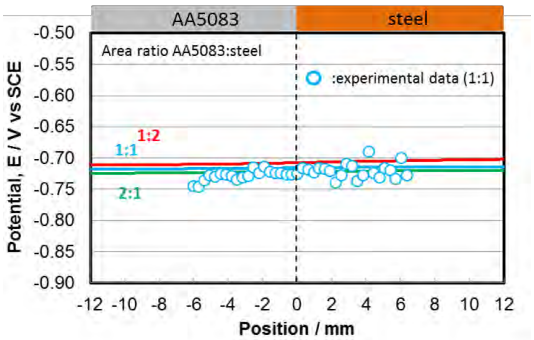

Figure 4 Potential distribution under 1.0mm thick of 0.6MNaCl solution.

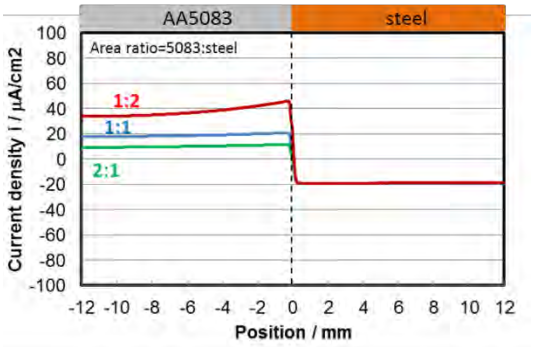

Figure 5 Current density distribution under 1.0mm thick of 0.6MNaCl solution.

Fig.6 shows the result of model calculation on the potential distribution under a 0.3 and 0.2 mm thick layers of 0.6M NaCl solution. The data taken from SKP under a 0.1mm thick is also plotted in this Figure. The difference in potential between the AA5083 and the steel became larger with decreasing thickness of electrolyte. In this study, we have not obtained the computational result for a 0.1mm thick electrolyte, because the calculation would not converge. Although the model results cannot be compared with experimental data under the same condition, the dependency of the thickness of electrolyte on the potential distribution was reasonable.

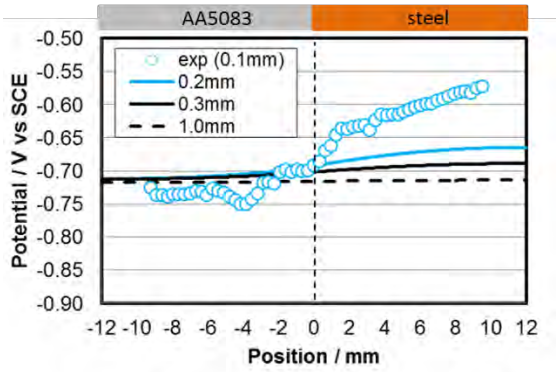

Figure 6 Potential distribution under thin 0.6MNaCl solution.

Fig.7 shows the result of the model calculations for the current density distribution under the thin 0.6M NaCl solution. The current distribution became wider with decreasing thickness of electrolyte as well. The area around the boundary seemed to be the most attacked. The peak current around the boundary under 0.2mm

thick was almost 10 times higher than that in bulk solution.

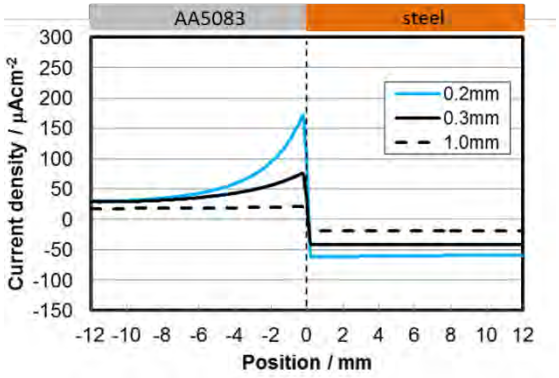

Figure 7 Current density distribution under thin 0.6MNaCl solution.

5. Discussion

The large difference in potential and current distributions can be seen between thin electrolyte and bulk solution in both model and experiment. The potential distribution in bulk solution was limited, because the geometry leads to a low resistance between the anode and cathode. On the other hand, wider distribution can be seen in the anodic current density on AA5083 under thin electrolyte. The, current density around the boundary was especially high. In this case, the high current density was limited to the vicinity of the boundary, because the thin electrolyte leads to a high resistance, inhibiting current passing to the area far away from the boundary.

The model calculation of the potential under thin electrolyte conditions had similar behavior to that observed in the experimental results. Therefore, this model may provide opportunities to predict atmospheric corrosion behavior. If the potential distribution in a range of the conditions can be obtained from the model, corrosion rate or corrosion damage can be predicted by comparing with the electrochemical data.

The reason why the calculation will not converge for electrolyte thickness less than 0.2mm will be analyzed. It is considered that mesh should be optimized to solve this problem. In addition, other factors including the chemical species, parameters in reaction term and so on will be analyzed.

Additional future work will consider the influence of sensitization of the alloy. The model was built based on the electrochemical properties of AA5083 with low sensitization in this study. However, severe corrosion mainly occurs on sensitized AA5083. In order to predict the corrosion of sensitized AA5083, it will be necessary to obtain appropriate boundary conditions from electrochemical measurements.

6. Conclusions

The preliminary model for predicting the galvanic corrosion between AA5083 and steel under atmospheric condition was built using Nernst-Plank module. The model calculation has good agreement with the experimental data in bulk solution and thin electrolyte. The model explains obviously the influence of area ratio and the thickness of electrolyte on the distribution of potential and current density.

7. Reference

1. L. Chen, X. Wang, R. G. Kelly, D. E. Brown, *Abstract #1273, 218th ECS Meeting LasVegas, NV, The Electrochemical Society*, (2010).
2. N. Murer, N. Missert, R. Buchheit, *Proceeding of the COMSOL Users Conference, Boston*, (2008).
3. N. Murer, R. Oltra, B. Vuillrmin, O. Neel, *Corrosion Science*, **52**, p130(2010).
4. R. Oltra, A. Zimmer, C. Sorriano, F. Rechou, C. Borkowski, O. Neel, *Electrochimica Acta*, **56**, p7038(2011).
5. M. Stratmann and H. Streckel, *Corrosion Science*, **30,** p681(1990).
6. G. Grundmeier, W. Schmidt, M. Stratmann, *Electrochimica Acta,* **45**, p2515(2000).
7. G. S. Frankel, M. Stratmann, M. Rohwerder, A. Michalik, B. Maier, J. Dora, M. Wicinski, *Corrosion Science*, **49,** p2021(2007).

8. Acknowledgements

This work is funded by the Office of Naval Research Grant N000140810315 with Dr. Airan Perez as Scientific Officer. We would like to recognize the assistance given by JFE Steel Corporation.